Parametric Study of an Early Stage of Alloy Solidification

Chittin Tangthieng
Department of Mechanical Engineering, Faculty of Engineering, Chulalongkorn University, Pyathai Road, Patumwan, Bangkok, 10300, Thailand
E-mail: fmectt@eng.chula.ac.th

Abstract

In the early stage of alloy solidification, the thicknesses of the solidified and mushy layers are theoretically and numerically investigated in this paper. The system under consideration is one dimensional and transient. The energy equations for four separate regions, i.e., wall, solid, mushy, and liquid regions, are formulated. A supplement equation, which relates the local temperature and the solid fraction, is included to close the governing system. Similarity variables are introduced to transform the governing equations to a set of ordinary differential equations. A combination of the fourth-order Runge-Kutta and the Secant iterative technique is employed to obtain the solutions. The effects of six dimensionless controlling parameters on the thicknesses of the solidified and mushy layers, written in terms of the solidification constants, are examined.

Keywords: alloy solidification, heat transfer, numerical method, parameter

1. Introduction

Many mathematical models for alloy solidification have been developed for the past decades by many researchers to predict the behavior of alloy solidification. It was found that these models were derived by either the mixture theory [1,2] or the volume-average approach [3]. However, the difficulty of how to develop these mathematical models originated from the complexity of the mushy region where the solid and liquid can coexist in equilibrium over a range of temperature. The characteristic length scale of the solid structure surrounded by the liquid phase (i.e., dendrite) is on the order of 10^{-5} to 10^{-4} m. As a result, utilizing the direct numerical simulation (DNS) by refining enough number of grids to obtain the microscopic details, is not plausible. Thus, an averaging procedure must be applied to the governing equation, leading to unknown quantities similar to the average Navier-Stokes equation for the turbulent flow. Each unknown quantity requires a separate model, such as the expression of the solid fraction [4], the viscosity model [5], the expression for the interfacial terms [3], and more sophisticated microscopic models [6].

The mathematical models developed by the volume-average approach can be solved by finite-element/volume methods. However, in the early stage of solidification where the solidified layer is thin compared to the wall thickness, the governing system can be transformed to a set of ordinary differential equations (ODE) by the similarity method [7]. Under this asymptotic condition, the thicknesses of the solidified layer and the liquidus isotherm are proportional to the square root of immersion time. The constants of the proportionality are referred to as the solidification constants, which can be determined by the combination of the fourth-order Runge-Kutta and the Secant iterative techniques. The effects of the dimensionless controlling parameters, appearing in the governing system, on the solidification constants are determined.

2. Problem Formulation

Figure 1 depicts the system under consideration in the present study. T_o, T_1, T_2, and T_∞ represent the initial wall temperature, the solidus temperature, the liquidus temperature, and the ambient melt temperature, respectively (i.e., $T_o < T_1 < T_2 < T_\infty$). δ_1 is the thickness of the solidified layer, and δ_2 is the location corresponding to the liquidus isotherm. δ_1 and δ_2 are also referred to as the solidus and liquidus lines, respectively. The region bound between δ_1 and δ_2 is the mushy region, where the solid fraction, ε, is equal to unity at $y = \delta_1$ and decreases to zero at $y = \delta_2$. Thus, $\delta_2-\delta_1$ represents the thickness of the mushy region.

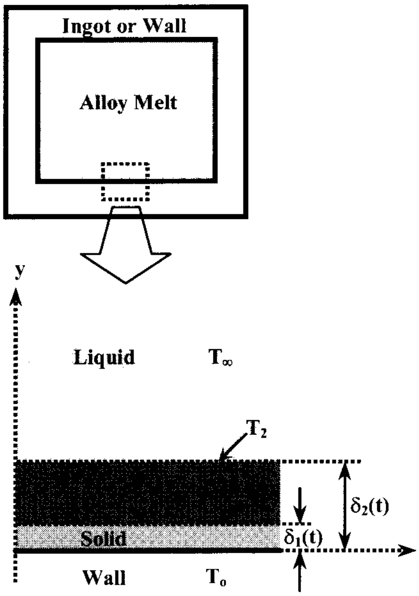

Figure 1: Schematic of the System under Consideration

To formulate the governing equations, major assumptions are made as follows: [1] The system is one dimensional and transient. [2] In the early stage of solidification, δ_1 and δ_2 are relatively thin compared to the wall thickness. Thus, the wall is assumed semi-infinite. [3] Physical properties of each phase are assumed constant whereas the physical properties of the mushy region can be determined by taking an average of each individual phase. However, the effects of the changes of the density and the specific heat within the mushy region are small compared to that of the thermal conductivity [8]. Therefore, the density and the specific heat of the solid, liquid, and mushy regions are treated as identical. On the other hand, the thermal conductivity of the mushy region is defined by taking an average of the thermal conductivity of each individual phase [1]:

$$k_m = (1-\varepsilon)\, k_\ell + \varepsilon\, k_s \tag{1}$$

[4] Convection in the liquid and mushy regions is negligible. [5] Local thermodynamic equilibrium exists. Hence, the solid fraction can be directly determined from the equilibrium phase diagram. [6] The concentration of the mixture does not change during the solidification process.

With these assumptions, the governing system can be written as follows:

(i) Wall region:

$$\rho c_p \frac{\partial T_w}{\partial t} = k_w \frac{\partial^2 T_w}{\partial y^2} \tag{2}$$

$$t = 0: T_w = T_o \tag{3-a}$$

$$y = 0: T_w = T_s \text{ and } k_w \frac{\partial T_w}{\partial y} = k_s \frac{\partial T_s}{\partial y} \tag{3-b}$$

$$y \to -\infty: T_w = T_o \tag{3-c}$$

(ii) Solid region:

$$\rho c_p \frac{\partial T_s}{\partial t} = k_s \frac{\partial^2 T_s}{\partial y^2} \tag{4}$$

$$t = 0: \delta_1 = 0 \tag{5-a}$$

$$y = 0: T_s = T_w \text{ and } k_s \frac{\partial T_s}{\partial y} = k_w \frac{\partial T_w}{\partial y} \tag{5-b}$$

$$y = \delta_1: T_s = T_1 \text{ and } \frac{\partial T_s}{\partial y} = \frac{\partial T_m}{\partial y} \tag{5-c}$$

(iii) Mushy region:

$$\rho c_p \frac{\partial T_m}{\partial t} = \frac{\partial}{\partial y}\left(k_m \frac{\partial T_m}{\partial y}\right) + \rho \Delta H \frac{\partial \varepsilon}{\partial t} \tag{6}$$

$$t = 0: \delta_2 = 0 \tag{7-a}$$

$$y = \delta_1: T_m = T_1 \text{ and } \frac{\partial T_m}{\partial y} = \frac{\partial T_s}{\partial y} \tag{7-b}$$

$$y = \delta_2: T_m = T_2 \text{ and } \frac{\partial T_m}{\partial y} = \frac{\partial T_\ell}{\partial y} \tag{7-c}$$

(iv) Liquid region:

$$\rho c_p \frac{\partial T_\ell}{\partial t} = k_l \frac{\partial^2 T_\ell}{\partial y^2} \tag{8}$$

$$t = 0: T_l = T_\infty \tag{9-a}$$

$$y = \delta_2: T_l = T_2\,, \text{ and } \frac{\partial T_l}{\partial y} = \frac{\partial T_m}{\partial y} \tag{9-b}$$

$$y \to \infty: T_\ell = T_\infty \tag{9-c}$$

It can be seen that the temperatures of each region are the primary unknowns of the governing system. However, the solid fraction must be written as a function of the local temperature. In order to do so, the equilibrium phase diagram as shown in Figure 2 is included to close the governing system.

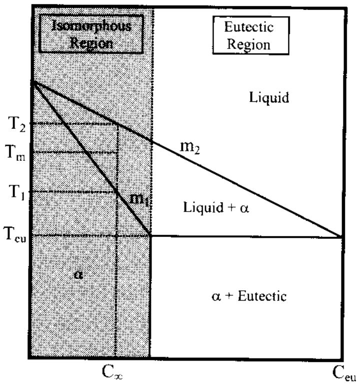

Figure 2: Equilibrium Phase Diagram

In this study, the category of alloy solidification is limited to the isomorphous system where both constituents of the binary alloy are completely miscible in both liquid and solid phases. As depicted in Figure 2, the isomorphous region is presented by the shaded area. For simplicity, the liquidus and solidus lines are assumed to be straight lines [9]. Thus, the relation between the solid fraction and the local temperature is given by

$$\varepsilon = \frac{T_2 - T_m}{(T_2 - T_m) + \kappa(T_m - T_1)} \tag{10}$$

Note that the above expression can be derived by applying the lever rule to the equilibrium phase diagram.

3. Mathematical Analysis

To perform a similarity transformation, similarity variables are introduced:

(i) Wall region:

$$\eta_w = \frac{y}{\sqrt{\alpha_w t}} \; ; \quad -\infty \le \eta_w \le 0$$
$$\theta_w = \frac{T_w - T_o}{T_1 - T_o} \; ; \quad 0 \le \theta_w \le \theta_w(0) \tag{11}$$

(ii) Solid region:

$$\eta_s = \frac{y}{\delta_1} \; ; \quad 0 \le \eta_s \le 1$$
$$\theta_s = \frac{T_s - T_o}{T_1 - T_o} \; ; \quad \theta_w(0) = \theta_s(0) \le \theta_s \le 1 \tag{12}$$

(iii) Mushy region:

$$\eta_m = 1 + \frac{y - \delta_1}{\delta_2 - \delta_1} \; ; \quad 1 \le \eta_m \le 2$$
$$\theta_m = 1 + \frac{T_m - T_1}{T_2 - T_1} \; ; \quad 1 \le \theta_m \le 2 \tag{13}$$

(iv) Liquid region:

$$\eta_\ell = 1 + \frac{y}{\delta_2} \; ; \quad 2 \le \eta_\ell \le \infty$$
$$\theta_\ell = 2 + \frac{T_\ell - T_2}{T_\infty - T_2} \; ; \quad 2 \le \theta_\ell \le 3 \tag{14}$$

The solidus and liquidus lines (δ_1 and δ_2) can be written in terms of σ_1 and σ_2 or the solidus and liquidus constants, respectively, as follows:

$$\delta_1 = \sigma_1 \sqrt{\alpha_s t} \tag{15}$$

$$\delta_2 = \sigma_2 \sqrt{\alpha_s t} \tag{16}$$

Substituting the similarity variables from equations (11)-(16) into equations (2)-(9) gives:

(i) Wall region:

$$\theta_w'' + \frac{\eta_w}{2}\theta_w' = 0 \tag{17}$$

$$\eta_w = 0 : \theta_w = \theta_s \text{ and } \theta_w' = \frac{R_{th}}{\sigma_1}\theta_s' \tag{18-a}$$

$$\eta_w \to -\infty : \theta_w = 0 \tag{18-b}$$

(ii) Solid region:

$$\theta_s'' + \frac{\sigma_1^2 \eta_s}{2}\theta_s' = 0 \tag{19}$$

$$\eta_s = 0 : \theta_s = \theta_w \text{ and } \theta_s' = \frac{\sigma_1}{R_{th}}\theta_w' \tag{20-a}$$

$$\eta_s = 1 : \theta_s = 1 \text{ and } \theta_s' = \frac{\sigma_1}{\sigma_2 - \sigma_1}\frac{1}{R_{sub}}\theta_m' \tag{20-b}$$

(iii) Mushy region:

$$\theta''_m+\left(\frac{R_k-1}{R_k\varepsilon+(1-\varepsilon)}\right)\left(\frac{\kappa}{Ste[(2-\theta_m)+\kappa(\theta_m-1)]^2}\right)(\theta'_m)^2$$
$$+\left(\frac{R_k}{R_k\varepsilon+(1-\varepsilon)}\right)\left(1+\frac{\kappa}{Ste[(2-\theta_m)+\kappa(\theta_m-1)]^2}\right)$$
$$\times\left(\frac{(\sigma_2-\sigma_1)^2}{2}\right)\left(\eta_m-1+\frac{\sigma_1}{\sigma_2-\sigma_1}\right)\theta'_m = 0 \tag{21}$$

$$\eta_m=1:\theta_m=1 \text{ and } \theta'_m=\frac{\sigma_2-\sigma_1}{\sigma_1}R_{sub}\theta'_s \tag{22-a}$$

$$\eta_m=2:\theta_m=2 \text{ and } \theta'_m=\frac{\sigma_2-\sigma_1}{\sigma_2}R_{sup}\theta'_\ell \tag{22-b}$$

(iv) Liquid region

$$\theta''_\ell + R_k\frac{\sigma_2^2}{2}(\eta_\ell-1)\theta'_\ell = 0 \tag{23}$$

$$\eta_\ell=2:\theta_\ell=2 \text{ and } \theta'_\ell=\frac{\sigma_2}{\sigma_2-\sigma_1}\frac{1}{R_{sup}}\theta'_m \tag{24-a}$$

$$\eta_\ell\to\infty:\theta_\ell=3 \tag{24-b}$$

The supplementary equation (10) can be written as a function of the dimensionless temperature as follows:

$$\varepsilon=\frac{2-\theta_m}{(2-\theta_m)+\kappa(\theta_m-1)} \tag{25}$$

It can be seen that the original partial differential equations are transformed to a set of ordinary differential equations. Six dimensionless parameters appearing in equations (17)-(25), namely the controlling parameters, are the solid-to-wall thermal ratio R_{th}, the solid-to-liquid thermal conductivity ratio R_k, the wall subcooling parameter R_{sub}, the liquid superheating parameter R_{sup}, the Stefan number Ste, and the equilibrium partition ratio κ. These controlling parameters are defined as:

$$R_{th}=\sqrt{\frac{k_s\rho c_p}{k_w\rho_w c_{pw}}},R_k=\frac{k_s}{k_\ell},R_{sub}=\frac{T_1-T_o}{T_2-T_1}, \tag{26}$$
$$R_{sup}=\frac{T_\infty-T_2}{T_2-T_1},Ste=\frac{c_p(T_2-T_1)}{\Delta H},\kappa=\frac{m_2}{m_1}$$

4. Numerical Solution Procedure

The temperature distribution of the wall and solid regions can be determined by direct integration of equations (17) and (19). The analytical solutions are given by:

$$\theta_w=\frac{R_{th}}{R_{th}+\mathrm{erf}(\sigma_1/2)}\left[1+\mathrm{erf}\left(\frac{\eta_w}{2}\right)\right] \tag{27}$$

$$\theta_s=\frac{R_{th}+\mathrm{erf}\left(\frac{\sigma_1\eta_s}{2}\right)}{R_{th}+\mathrm{erf}(\sigma_1/2)} \tag{28}$$

On the other hand, the temperature distribution of the mushy and liquid regions can be obtained numerically. The classical fourth-order Runge-Kutta method is selected to solve these two ordinary differential equations. The initial conditions are the values of θ_m and θ'_m at $\eta_m = 1$, which are given by equation (22-a). By utilizing the analytical solution of θ_s, i.e., equation (28), the value of θ'_m at $\eta_m = 1$ is:

$$\theta'_m(1)=\frac{(\sigma_2-\sigma_1)R_{sub}}{\sqrt{\pi}}\left[\frac{\exp(-\sigma_1^2/4)}{R_{th}+\mathrm{erf}(\sigma_1/2)}\right] \tag{29}$$

It should be noted that most of the transformed ordinary differential equations and associated boundary conditions in the mushy and liquid regions are functions of σ_1 and σ_2, which are unknowns. Thus, the numerical algorithm cannot be performed unless σ_1 and σ_2 have been determined. To eliminate this difficulty, the values of σ_1 and σ_2 are estimated first. The Secant iterative technique is applied to update σ_1 and σ_2 until these two values match the boundary conditions, i.e., $\theta_m(2) = 2$ and $\theta_m(\infty) = 3$. The solution is shown to converge if the differences between the values of σ_1 and σ_2 and the matching conditions are less than a prescribed tolerance of 10^{-8}. In addition, the grid-independent study of the numerical algorithm has already been examined in Reference [7].

5. Results and Discussion

In this study, the effects of the controlling parameters on σ_1 and σ_2 are determined. A set of the controlling parameters are selected as a reference case, which are $R_{th} = 0.3$, $R_k = 1$, $R_{sub} = 1$, $R_{sup} = 3$, Ste = 0.1, and $\kappa = 0.3$. These numbers are based on the physical properties of the Pb-10% wt Sn alloy and the temperature data in a round-off version [7]. In practice, R_{sub} and R_{sup} can be controlled by adjusting the initial wall temperature, T_o and the ambient melt temperature, T_∞, respectively. On the other hand, the rest of the controlling parameters, i.e., R_{th}, R_k, Ste, and κ, depend on selection of the wall and the freezing materials. The numerical experiments are preformed by varying one of the controlling parameters whereas the others are kept constant at the reference case.

Figure 3 depicts the variations of σ_1 and σ_2 with R_{th}. As R_{th} is decreased, σ_1 and σ_2 increase because of the higher heat capacity of the wall, resulting in a higher cooling effect from the wall to the melt. Unlike the values of σ_1 and σ_2, the thickness of the mushy region (i.e., $\sigma_2-\sigma_1$) is not a strong function of R_{th}. As R_{th} asymptotically approaches zero, the wall becomes isothermal with infinite heat capacity, which provides the highest cooling effect. On the other hand, when R_{th} is increased to a certain limit, which is approximately equal to 1.75, the wall heat capacity is not enough to generate the solidified layer on its surface. Thus, σ_1 approaches zero.

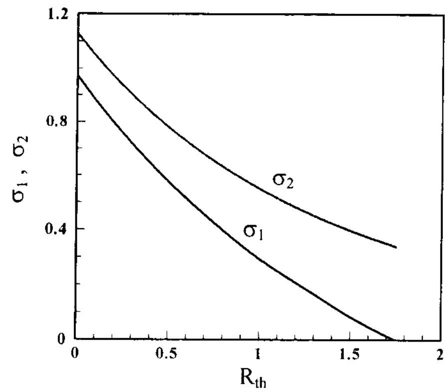

Figure 3: Variations of σ_1 and σ_2 with R_{th}

The effect of R_k on σ_1 and σ_2 is presented in Figure 4. σ_1 increases with increasing R_k. It is known that the higher value of the thermal conductivity of the solid phase, the faster the cooling effect can be absorbed by the melt, leading to the thicker solidified layer. On the other hand, σ_2 appears to be marginally sensitive to the change of R_k. As a result, the thickness of the mushy region, $\sigma_2-\sigma_1$ decreases as R_k is increased.

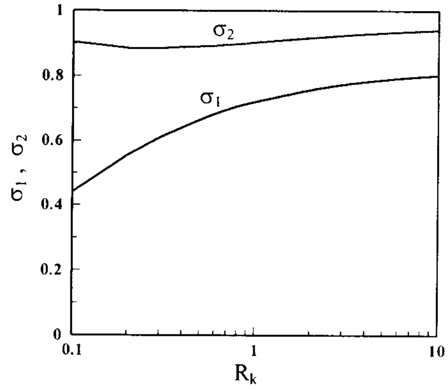

Figure 4: Variations of σ_1 and σ_2 with R_k

The variations of σ_1 and σ_2 with R_{sub} are illustrated in Figure 5. It can be seen that σ_1 and σ_2 increase with increasing R_{sub}. As expected, an increase of R_{sub} corresponds to lower values of T_o, causing higher values of σ_1 and σ_2. However, $\sigma_2-\sigma_1$ is a weak function of R_{sub}. As R_{sub} decreases toward 2.7, σ_1 decreases to zero due to the insufficient degree of wall subcooling.

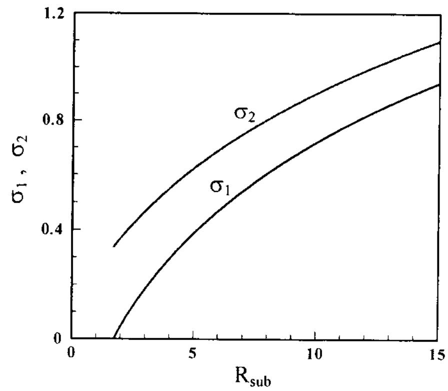

Figure 5: Variations of σ_1 and σ_2 with R_{sub}

Figure 6 depicts the effect of R_{sup} on σ_1 and σ_2. As R_{sup} is increased, σ_1 and σ_2 decrease. Physically, more heat is conducted from the melt to the wall as the ambient wall temperature (T_∞) is higher. It is noticed that the value of σ_1 reduces to zero if R_{sup} is raised to a certain limit, which is approximately equal to 30, because of the excess value of T_∞. If R_{sup} asymptotically approaches zero corresponding to the solidification at the liquidus temperature, σ_1 reaches the upper limit whereas σ_2 monotonically increases. Note that unlike R_{sub}, $\sigma_2-\sigma_1$ is a strong function of R_{sup} especially when $R_{sup} << 1$.

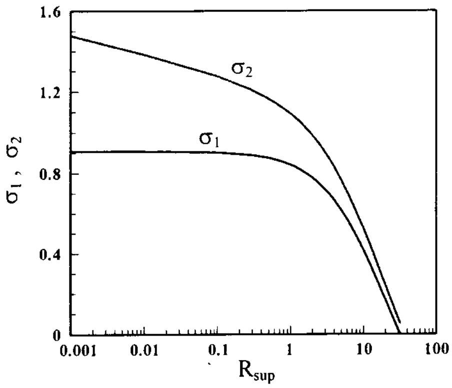

Figure 6: Variations of σ_1 and σ_2 with R_{sup}

The effect of Ste on $\sigma_2-\sigma_1$ is presented in Figure 7. Increasing Ste causes σ_1 and σ_2 to increase. A material with higher Ste has a smaller latent heat of fusion. Hence, under the same cooling condition, it will require less cooling effect from the wall in order to form a thicker solidified layer (or higher σ_1). It is found that $\sigma_2-\sigma_1$ is not sensitive to the change of Ste.

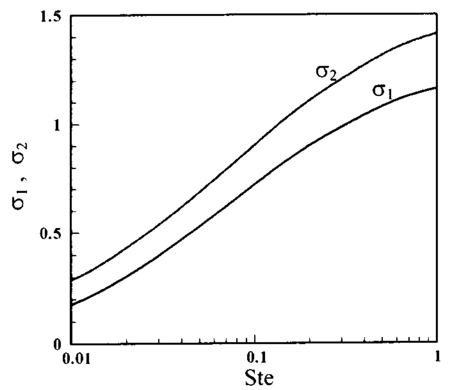

Figure 7: Variations of σ_1 and σ_2 with Ste

Figure 8 depicts the variations of σ_1 and σ_2 with κ. It can be seen that both σ_1 and σ_2 are weak functions of κ, especially for σ_1. By increasing κ from 0.1 to 0.7, which is the most common value of κ for a binary alloy, the values of σ_1 and σ_2 increase by 1.1 and 6.4 percent, respectively. Similar to σ_1 and σ_2, $\sigma_2-\sigma_1$ is also a very weak function of κ.

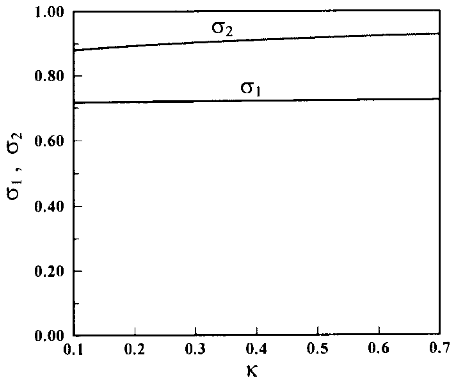

Figure 8: Variations of σ_1 and σ_2 with κ

6. Conclusions

In this present study, a parametric study of an early stage of alloy solidification has been performed. After utilizing the similarity transformation, the behavior of an early stage of the alloy solidification is characterized by the solidification constants, σ_1 and σ_2, which are functions of six dimensionless controlling parameters. The numerical results have been obtained by a combination of the fourth-other Runge-Kutta method and the Secant iterative technique. Based on the numerical results, the solidified layer, i.e.,σ_1, increases as either R_{sub}, R_k, or Ste is increased, but it decreases as either R_{th} or R_{sup} is increased. However, it appears to be insensitive to the change of κ. On the other hand, the thickness of the mushy region, i.e.,$\sigma_2-\sigma_1$, decreases as either R_k or R_{sup} is increased. It is a weak function of either R_{th}, R_{sub}, or Ste and insensitive to the change of κ.

7. Nomenclature

(i) Symbols

c_p = specific heat [J/kg-K]

ΔH = latent heat of freezing [J/kg]

k = thermal conductivity [W/m-K]

m = slope of a line in an equilibrium phase diagram

R_k = solid-to-liquid thermal conductivity ratio

R_{sub} = wall subcooling parameter
R_{sup} = liquid superheating parameter
R_{th} = solid-to-wall thermal ratio
Ste = Stefan number
t = time [s]
T = temperature [K]
y = spatial coordinate [m]

(ii) Greek Symbols
α = thermal diffusivity [m^2/s]
δ = thickness [m]
ε = solid fraction
η = similarity independent variable
κ = equilibrium partition ratio
ρ = density [kg/m^3]
σ = solidification constant
θ = dimensionless temperature

(iii) Subscripts
o = initial state
1 = solidus temperature or solidus line
2 = liquidus temperature or liquidus line
l = liquid region
m = mushy region
s = solid region
w = wall region
∞ = ambient state

8. References

[1] Bennon, W. D. and Incropera, F. P., A Continuum Model for Momentum, Heat and Species Transport in Binary Solid-liquid Phase Change Systems-I Model Formulation, Int. J. Heat Mass Transfer, Vol. 30, pp. 2161-2170, 1987.

[2] Voller, V. R., Brent, A. D., and Prakash, C., The Modelling of Heat, Mass and Solute Transport in Solidification Systems, Int. J. Heat Mass Transfer, Vol. 32, pp. 1718-1731, 1989.

[3] Ni, J. and Beckermann, C., A Volume-Averaged Two-Phase Model for Transport Phenomena during Solidification, Metall. Trans. B, Vol. 22B, pp. 339-361, 1991.

[4] Beckermann, C. and Viskanta, R., Double-Diffusive Convection during Dendritic Solidification of a Binary Alloy, PhysicoChem. Hydro., Vol. 10, pp. 195-213, 1988.

[5] Krieger, I. M., Rheology of Monodisperse Lactices, Adv. Colloid. Interface Sci., Vol. 3, pp. 111-126, 1972.

[6] Wang, C. Y. and Beckermann, C., Equiaxed Dendritic Solidification with Convection: Part I Multiscale/Multiphase Modeling, Metall. Mater. Trans. A, Vol. 27A, pp. 2754-2764, 1996.

[7] Tangthieng, C., A Numerical Study of an Early Stage of Alloy Solidification Using Similarity Transformation and Secant Iterative Technique, Paper no. MM11 Proceeding of the 17th Conference on Mechanical Engineering Network of Thailand, Prachinburi, 15-17 October, 2003.

[8] Stevens, R. and Poulikakos, D., Freeze Coating of a Moving Substrate with a Binary Alloy, Numer. Heat Transfer Part A, Vol. 20, pp. 409-432, 1991.

[9] Kurz, W. and Fisher, D. J., Fundamentals of Solidification, 3rd Edition, Trans Tech, Switzerland, pp. 15-16, 1989.